Dynamics of micromagnetic measurements

Ivo Klik, Ching-Ray Chang, and Huei-Li Huang
Department of Physics, National Taiwan University, Taipei, Taiwan, Republic of China
(Received 23 October 1992)

The response of a micromagnetic system to changes in ambient temperature or applied field is studied as a function of the overbarrier relaxation rate and of the intermediate nonequilibrium states through which the system is passing. We first derive an equation for the thermomagnetic curve and the corresponding time-dependent dc susceptibility. Next we write down an equation for the hysteresis loop and discuss its applications to calculation of the frequency and temperature-dependent coercivity. In conclusion we present a model calculation of the switching-field distribution for a system of noninteracting uniaxial particles. Both the reversible and irreversible susceptibility are recovered from our results as limiting cases.

I. INTRODUCTION

Observed properties of small, single domain ferromagnetic particles depend strongly on the measurement duration: The outcome of an observation whose waiting time is much larger [e.g., vibrating-sample magnetometer (VSM) or SQUID] than the intrinsic magnetization switching time differs radically from what one obtains if the system cannot relax appreciably while under observation (e.g., in Mössbauer spectroscopy). For this reason the concept of blocking temperature T_B was introduced.[1] T_B is defined as the temperature at which the decay rate of the system is $\Gamma=10^{-2}$ Hz. Above T_B the particle by assumption switches freely on the measurement time scale while below T_B its magnetization remains blocked at a local energy minimum. The blocking temperature model has proved very successful in applications but a more realistic description bridging the gap between the two regimes is clearly called for. We consider therefore the response of a particle ensemble to some change in its environment affecting its relaxation properties. Our aim is to give an analytic expression for the time evolution of the probability distribution function and thence to derive the time-dependent nonequilibrium magnetization and susceptibility. These quantities are given in terms of the overbarrier decay rate Γ, the equilibrium properties of the system, and of all its past history. The regime obtained below T_B is recovered if the past persists, either because of low temperature or short observation time. Obversely, in the high-temperature limit the past is "forgotten" and has no bearing on the present.

We study first the initial thermomagnetic curve[2-4] of an array of noninteracting single domain particles within the coherent rotation model. We consider two kinds of measurement distinguished by their history. In the first kind (direct transition measurement) the system finds itself initially in a disordered demagnetized state in zero field at some low temperature T_0 well below the Curie point T_C. Then an external magnetic field is turned on and the temperature is raised to $T<T_C$, both of these changes occurring so rapidly that the initial state persists until the observation temperature T is attained. We introduce here some basic definitions and proceed then to study the case where temperature is being raised gradually at a constant, finite rate (sequential transition measurement). In either evolution mode we write down an equation for the thermomagnetic curve, derive an expression for the time-dependent dc susceptibility, and discuss their limits of validity. The model also finds application in the theory of cluster spin-glass alloys.[5,6]

From a practical point of view, the dynamic response of ferromagnetic particles to the time-varying magnetic field[7-9] is of far greater importance than the thermomagnetic curve and we therefore apply our theory also to gradual changes in magnetic field and derive an equation for the hysteresis loop. At the end of Sec. IV, we then discuss our calculations of the coercivity[10-12] of an array of noninteracting particles and also some further applications of our theory. Finally, in Sec. V we present a numerical calculation of the frequency and temperature-dependent switching field distribution of such an array. The well-known high- (purely reversible) and low-temperature (purely irreversible) limits are recovered from our results.

Let us yet establish some basis definitions. Unless otherwise specified we assume[2-4] that below T_C both the saturation magnetization M_s and anisotropy constants $K^{(n)}$ are temperature dependent:

$$M_s(\tau)=M_s(0)(1-\tau)^{1/3}\ , \tag{1}$$

$$K^{(n)}(\tau)\propto[M_s(\tau)M_s^{-1}(0)]^{n(n+1)/2}\ , \tag{2}$$

where $\tau=T/T_c\leq 1$ is the reduced temperature. In particular, for the first nonvanishing anisotropy constant we obtain $K^{(2)}\equiv K(\tau)=K(0)(1-\tau)$. Within the model of coherent rotation we parametrize the magnetization vector $\mathbf{M}$ in terms of the variables[13,14] (p,ϕ), $p=\cos\theta\in(-1,1)$ and $\phi\in\langle 0,2\pi)$, and the integral over this domain is designated as Tr. If α_i are direction cosines then, in this parametrization,

$$\mathbf{M}=M_s[(1-p^2)^{1/2}\cos\phi,(1-p^2)^{1/2}\sin\phi,p\,] =M_s\boldsymbol{\alpha}\ . \tag{3}$$

Further let $\mathbf{m}=v\mathbf{M}$ be the magnetic moment of a particle of volume V with magnetization $\mathbf{M}$ and let also $\langle x\rangle_\tau$ be the thermal average of x at temperature τ. We set $k_B=1$ throughout.

II. THERMOMAGNETIC CURVE UNDER DIRECT TRANSITION

For definiteness we initially base our qualitative discussion of the direct transition measurement on a model system consisting of only two noninteracting uniaxial particles whose easy axes are oriented either along the three or one direction. At $t<0$ the system is in a demagnetized state at some low temperature $\tau_0<1$. At $t=0$, a constant magnetic field $B>0$ is applied in the three direction and at the same time temperature is increased to $\tau>\tau_0$. The energy of either one of the two particles becomes

$$E=KV[1-2b\alpha_3-(\alpha_3\cos\psi-\alpha_1\sin\psi)^2]\ , \tag{4}$$

where $\psi=0$ for the parallel particle whose easy axis is in the three direction or $\psi=\pi/2$ for the perpendicular particle. At $t<0$ the parallel particle has two equivalent equally populated minima at $\alpha_3=p=\pm1$ separated by a barrier at $p=0$; the biasing action of the field shifts the barrier to the point $p=-b(\tau)$ where

$$b(\tau)=\frac{BM_s}{2K}=\beta(1-\tau)^{-2/3}\le 1\ . \tag{5}$$

In this definition $\beta=BM_s(0)/[2K(0)]=B/B_N(0)$ is a reduced applied field and $B_N(0)$ is a nucleation field at $T=0$. The two barrier heights are then $Q_\pm(\tau)=VK(\tau)[1\pm b(\tau)]^2$. To every $\beta<1$ there exists a volume-independent critical temperature τ_β,

$$\tau_\beta=1-\beta^{3/2}\ , \tag{6}$$

at which $b(\tau_\beta)=1$ and the barrier vanishes. This temperature thus heralds the onset of approximately reversible behavior and we assume that for $\tau\ge\tau_\beta$ the particle is in thermal equilibrium at all times. The perpendicular particle exhibits this reversible behavior only: The two equivalent minima initially at points (0,0) and $(0,\pi)$ shift at $\tau<\tau_\beta$ to $(b,0)$ and (b,π) yielding nonzero net magnetization. There is no bias and no thermally driven overbarrier flux since, by assumption, the two minima are equally populated. At $\tau=\tau_\beta$ these two minima merge. Our two particles thus represent the extremes of stationary (thermal equilibrium) and nonstationary behavior, any other alignment of the axes leads to a combination of the described processes. Stationary effects place the peak of the thermomagnetic curve to the temperature τ_β. Overbarrier relaxation, with net rate $\Gamma(\tau,\beta)$, results in a shift of the peak towards lower temperatures and the magnitude of this shift increases with increasing waiting time t.

Now let $P(\tau,\beta)$ be a normalized equilibrium distribution function. Within the approximation of decay rate theory, at *constant* τ and β, the time-dependent probability distribution $\bar{P}$ evolves in time as

$$\bar{P}(\tau,\beta|t,0)=P_{t=0}e^{-\Gamma(\tau,\beta)t}+(1-e^{-\Gamma(\tau,\beta)t})P(\tau,\beta)\ . \tag{7}$$

This formula[15] is obtained by replacing the relevant Fokker-Planck equation by $\dot{q}=-\Gamma q$, $q=\bar{P}-P(\tau,\beta)$. There is $P_{t=0}=P(\tau_0,0)$ by assumption and the time-dependent projection of the mean magnetic moment of the parallel particle into the field direction is

$$\bar{m}_\parallel^{(3)}(\tau,\beta|t,0)=\begin{cases}(1-e^{-\Gamma t})\langle m_\parallel^{(3)}\rangle_\tau\ , & \tau<\tau_\beta\ ,\\ \langle m_\parallel^{(3)}\rangle_\tau\ , & \tau\ge\tau_\beta\ ,\end{cases} \tag{8}$$

where the static average

$$\langle m_\parallel^{(3)}\rangle_\tau=M_s(\tau)V\cdot\mathrm{Tr}\{pP_\parallel(\tau,\beta)\}\ .$$

The initial demagnetized state $P_{t=0}$ does not contribute to $\bar{m}_\parallel^{(3)}$. For $t>0$ the function $\bar{m}_\parallel^{(3)}$ is discontinuous at $\tau=\tau_\beta$ but in this temperature region the exponent is negligible for any time of interest. The perpendicular particle satisfies $\bar{m}_\perp^{(3)}(\tau,\beta|t)\equiv\langle m_\perp^{(3)}\rangle$ at all times. For the time-dependent dc susceptibility of the parallel particle we obtain

$$\bar{\chi}_\parallel(\tau,\beta|t,0)=\frac{1}{V}\left\langle\frac{\partial m_\parallel^{(3)}}{\partial B}\right\rangle_\tau=\begin{cases}\chi_\parallel(\tau,\beta)(1-e^{-\Gamma t})+\langle M_\parallel^{(3)}\rangle_\tau(\partial\Gamma/\partial B)te^{-\Gamma t}\ , & \tau<\tau_\beta\ ,\\ \chi_\parallel(\tau,\beta)\ , & \tau\ge\tau_\beta\ ,\end{cases} \tag{9}$$

where the static dc susceptibility

$$\chi_\parallel(\tau,\beta)=(T)^{-1}\{\langle[M_\parallel^{(3)}]^2\rangle_\tau-\langle M_\parallel^{(3)}\rangle_\tau^2\}\ .$$

Within the blocking temperature theory, Eq. (9) was given previously by Gittelman[16] without the anomalous term originating in change of decay rate with field. The Fourier transform $\mathcal{F}[\bar{\chi}](\omega)$ has Drude form,[6,16] but Eq. (9) describes a nonlinear response to the applied dc field which depends on the time t elapsed during measurement and has no relation to an external ac field of frequency ω. The peak of $\bar{\chi}(\tau)$ shifts to lower temperatures with increasing t and is therefore *not* located at the boundary between reversible and irreversible behavior, i.e., at τ_β, which is often interpreted as spin-glass temperature. In the perpendicular particle there is no overbarrier decay at any temperature and its susceptibility $\chi_\perp(\tau,\beta)$ is static at all times. The high-temperature limit of $\chi_\perp$ and $\chi_\parallel$ is given by the usual Langevin formula $\chi_\parallel\sim\chi_\perp\sim M_s^2V/(3T)$ as $KV/T\to0$ while the low-temperature limit yields the often quoted[5,16] results $\chi_\perp\sim M_s^2/(2K)$, $\chi_\parallel=O(T/V)$ as $KV/T\to\infty$.

The simple formulas (7)–(9) hold for evolution at constant τ and β (direct transition measurement) but they are *approximately* valid also for sequential measurements provided that the barrier height is very large so that a small change in temperature leads to a large change in the Arrhenius factor $\exp(-Q/T)$. Thus, as the temperature is gradually raised the initial disordered state persists

until some critical temperature at which relaxation effects on the time scale of the measurement set in. Thermal equilibrium is then attained over a narrow temperature interval and Eqs. (7)–(9) approximately hold. We shall encounter a similar situation in Sec. V where we discuss coercivity at very low temperatures.

Let us list now some generalizations and possible applications of our simple two-particle model. The most trivial generalization is achieved by allowing for volume variation within the sample. The volume and thermal averages are carried out independently and the resultant thermomagnetic curve is a superposition of curves with various waiting times. Thus, for $BaFe_{12}O_{19}$ particles of mean size 10^{-7} m, Popov *et al.*[3] report a maximum close to τ_β and apparently little affected by thermal activation introduced into their numerical simulation only as a refinement of the reversible process. On the other hand, Chien *et al.*[17] found in Fe-SiO_2 the peak shifted to temperatures $\tau \approx \tau_\beta/3$ for Fe particles of size 10^{-8} m. Here the overbarrier mechanism dominates and the direct transition model is no longer applicable; the shift of the peak and the relaxation process extending over a large temperature interval can, however, be described by means of the sequential transition model treated in the next section. Further applications: Angular distribution of the particles [$0 \le \psi \le \pi/2$ in Eq. (4) for E] is easily taken into account since formulas (8)–(9) still hold, but τ_β can in this case only be found numerically the same as for particles of more complex symmetry. An important exception is provided by cubic systems in an external field parallel to one of the easy axes where the nucleation field is known.[13] For Fe-type particles, $K^{(2)}=0$ and $K^{(4)}>K^{(6)}>0$, there exist two nucleation fields. At $B<B_{N_1}\approx 0.544K^{(4)}/M_s$, the decay proceeds in two stages: First from the metastable minimum at $p=1$ into the four equivalent minima initially in the (0,0,1) plane and then to $p=-1$. At $B_{N_1}\le B<B_{N_2}=2K^{(4)}/M_s$, the decay proceeds directly from $p=1$ into -1. By virtue of Eqs. (1) and (2) the critical fields decrease rapidly with temperature, $B_{N_j}\propto(1-\tau)^3$. For Ni-type cubic symmetry ($K^{(4)}<0$) there exists but one nucleation field $B_N=4(K^{(4)}-K^{(6)}/3)/(3M_s)$ which decreases uniformly with τ.

III. THERMOMAGNETIC CURVE UNDER SEQUENTIAL TRANSITION

The merit of the direct transition model lies in the simple time evolution law (7)–(9) but in experiments the initial disordered state is usually heated up gradually (zero-field cooling) and, as discussed above, the initial disordered state does not necessarily relax over a narrow temperature interval. We therefore address now the sequential measurement in which the external field is held constant at times $t>t_0=0$ while the temperature is being raised at a uniform rate ρ^{-1}, $dt=\rho d\tau$. We trace the following sequence of events: At $t\le t_0$, the system is in thermal equilibrium in zero field, $P_{\rm in}=P(\tau_0,0)$. At $t=t_0$, a magnetic field β is turned on and the system is allowed to relax towards the new equilibrium state $P(\tau_0,\beta)$ for a time period Δt. At $t_1=t_0+\Delta t$, the temperature is raised to $\tau_1=\tau_0+\Delta\tau$ and again the system is allowed to relax towards $P(\tau_1,\beta)$ at this temperature for a time Δt after which the temperature is raised anew. We may therefore schematically write

$$P_{\rm in}\xrightarrow{\tau_0}\bar{P}(\tau_0|t_1,t_0)\xrightarrow{\tau_1}\bar{P}(\tau_1|t_2,t_1)\xrightarrow{\tau_2}\cdots\xrightarrow{\tau_n}\bar{P}(\tau_n|t_{n+1},t_n)\ ,$$

where for simplicity of notation we omit the β dependence of $\bar{P}$ written out explicitly in Eq. (7). The values of τ_i above the arrows show at what temperature the relaxation is taking place. At constant temperature we may use Eq. (7) on every subinterval and write down the sequence

$$\begin{aligned}
&\bar{P}(\tau_0,\beta|t_1,t_0)=P_{\rm in}e^{-\Gamma_0\Delta t}+(1-e^{-\Gamma_0\Delta t})P_0\ ,\\
&\bar{P}(\tau_1,\beta|t_2,t_1)=\bar{P}(\tau_0,\beta|t_1,t_0)e^{-\Gamma_1\Delta t}+(1-e^{-\Gamma_1\Delta t})P_1\ ,\\
&\qquad\vdots\\
&\bar{P}(\tau_n,\beta|t_{n+1},t_n)=\bar{P}(\tau_{n-1},\beta|t_n,t_{n-1})e^{-\Gamma_n\Delta t}\\
&\qquad\qquad+(1-e^{-\Gamma_n\Delta t})P_n\ .
\end{aligned}\tag{10}$$

Successive substitutions then yield

$$\tilde{P}(\beta|t_{n+1},t_0)=(P_{\rm in}-P_0)e^{-\gamma_{0,n}\Delta t}+\sum_{j=1}^{n}(P_{j-1}-P_j)e^{-\gamma_{j,n}\Delta t}+P_n \tag{11}$$

for the normalized distribution function $\tilde{P}$ evolving from $P_{\rm in}$ in constant field and at uniformly varying temperature. We introduced here the function $\gamma_{m,n}=\sum_{i=m}^{n}\Gamma_i$ and wrote $\Gamma_i=\Gamma(\tau_i,\beta)$ and $P_i=P(\tau_i,\beta)$ for brevity. The distribution function at $\tau=\tau_n$ is therefore a superposition of the equilibrium distributions P_i, $i\le n$, the most recent ones having decayed least. Their relative abundance at $\tau=\tau_n$ depends on the functional form of $\Gamma(\tau,\beta)$, i.e., on the set $\{\Gamma_i\}_{i\in\langle 0,n-1\rangle}$. In the limit $\Delta t\to 0$, Eq. (11) becomes

$$\tilde{P}(\beta|t,t_0)=[P_{\rm in}-P(\tau_0,\beta)]e^{-\rho\gamma(\tau,\tau_0)}+P(\tau,\beta)-\int_{\tau_0}^{\tau}d\tau'\frac{\partial P}{\partial\tau'}e^{-\rho\gamma(\tau,\tau')}\ , \tag{12}$$

where $t=t_0+\rho(\tau-\tau_0)$ and the function γ is

$$\gamma(\tau,\bar{\tau})=\int_{\bar{\tau}}^{\tau}dx\,\Gamma(x,\beta)\ . \tag{13}$$

The first term in (12) represents the discontinuous transition due to the sudden switching on of the field. The derivatives of the normalized equilibrium distribution are conveniently calculated from the relation

$$\partial P/\partial\tau=\tau^{-2}[E-\langle E\rangle_\tau-\tau(E'-\langle E'\rangle_\tau)]P \ . \quad (14)$$

The total energy E depends on temperature via relations (1) and (2) and $E'=\partial E/\partial\tau$.

Given Eqs. (11) or (12) it is easy to write down expressions for the time-dependent magnetization $\tilde{m}$ and the dc susceptibility $\tilde{\chi}$ which replace Eqs. (8) and (9) in the irreversible domain $\tau<\tau_\beta$. The thermomagnetic curve becomes

$$\tilde{m}(\tau,\beta|t)=-\langle m\rangle_{\tau_0}e^{-\rho\gamma(\tau,\tau_0)} - \int_{\tau_0}^{\tau}d\tau'\frac{\partial\langle m\rangle_{\tau'}}{\partial\tau'}e^{-\rho\gamma(\tau,\tau')}+\langle m\rangle_\tau \ , \quad (15)$$

and the derivative of the equilibrium magnetic moment $\langle m\rangle_\tau$ is expressed as

$$\partial\langle m\rangle_\tau/\partial\tau=\tau^{-2}(\langle Em\rangle_\tau-\langle E\rangle_\tau\langle m\rangle_\tau) -\tau^{-1}(\langle E'm\rangle_\tau-\langle E'\rangle_\tau\langle m\rangle_\tau)+\langle m'\rangle_\tau \ . \quad (16)$$

In the last term $m'=\partial m/\partial\tau$ by virtue of Eq. (1). Observation results depend now on the sweep rate ρ^{-1}: In a fast sweep the system finds itself in effect blocked until some critical temperature at which thermal effects occur on the measurement time scale. This is the direct measurement limit recovered from Eq. (15) if $\gamma(\tau,\tau')\to\tau-\tau_0$ is independent of the intermediate temperatures. A very gradual sweep results in a large shift (and spread) of the peak due to increased reversal probability at lower temperatures. For the time-dependent dc susceptibility $\tilde{\chi}$ we obtain the relation

$$\tilde{\chi}(\beta|t,t_0)=-\langle M\rangle_{\tau_0}\frac{\partial}{\partial B}e^{-\rho\gamma(\tau,\tau_0)} -\int_{\tau_0}^{\tau}d\tau'\frac{\partial M(\tau')}{\partial\tau'}\frac{\partial}{\partial B}e^{-\rho\gamma(\tau,\tau')} -\chi(\tau_0)e^{-\rho\gamma(\tau,\tau_0)} -\int_{\tau_0}^{\tau}d\tau'\frac{\partial\chi(\tau')}{\partial\tau'}e^{-\rho\gamma(\tau,\tau')}+\chi(\tau) \ , \quad (17)$$

which replaces Eq. (9) at $\tau<\tau_\beta$. The derivative $\partial\gamma/\partial B$ depends on the studied model but the derivative of the static susceptibility χ may again be expressed in terms of averages. Let, for brevity, χ be written as $\chi(\tau)=\zeta(\tau)/(TV)$, where $\zeta=\langle m^2\rangle_\tau-\langle m\rangle_\tau^2$. Then

$$\partial\zeta/\partial\tau=\tau^{-2}[\langle Em^2\rangle_\tau-\langle E\rangle_\tau\langle m^2\rangle_\tau] -\tau^{-1}[\langle E'm^2\rangle_\tau-\langle E'\rangle_\tau\langle m^2\rangle_\tau] +2[\langle mm'\rangle_\tau-\langle m\rangle_\tau\partial\langle m\rangle_\tau/\partial\tau] \ . \quad (18)$$

This formula concludes our study of the thermomagnetic curve and time-dependent dc susceptibility. We wish again to emphasize that the position of their extrema reflects not only the intrinsic properties of the system, but also the mode of measurement. In the currently available micromagnets of size 10^{-7}–10^{-8} m this dependence becomes prominent and our equations may be used to separate the intrinsic and incidental components of observation data.

IV. THE HYSTERESIS LOOP

Within the Stoner-Wohlfarth theory the static hysteresis loop of a particle with uniaxial anisotropy, $E=E(p)$, is easily found from the conditions $dE/dp\equiv E_p=0$ and $E_{pp}\geq 0$. The astroid $\mathcal{A}^{(1)}$, so popular in applications, allows one to construct it by geometric means. Interestingly enough, an analogous two-parametric surface $\mathcal{A}^{(2)}$ exists in three dimensions. Let $E=-\mathbf{b}\cdot\boldsymbol{\alpha}(p,\phi)+f(p,\phi)$. The equations $E_p=E_\phi=\mathrm{Hess}(E)=0$ then yield $\mathcal{A}^{(2)}=\{b_1,b_2,b_3\}$, where

$$b_1(p,\phi)=-(1-p^2)^{-1/2}\{2\sin\phi f_\phi+\delta\cos\phi\}/2 \ , \quad (19)$$

$$b_2(p,\phi)=(1-p^2)^{-1/2}\{2\cos\phi f_\phi-\delta\sin\phi\}/2 \ , \quad (20)$$

$$b_3(p,\phi)=\{2f_p-p(1-p^2)f_{pp} -p(1-p^2)^{-1}[f_{\phi\phi}+D]\}/2 \ . \quad (21)$$

$$\delta=(1-p^2)^2f_{pp}+f_{\phi\phi}+D \ ,$$

$$D^2=4[(1-p^2)f_{\phi p}+pf_\phi]^2+[f_{\phi\phi}-(1-p^2)^2f_{pp}]^2 \ .$$

If $E_p=E_\phi=0$ then also $db_1/db_3=\tan\theta\cos\phi$ and $db_2/db_3=\tan\theta\sin\phi$ and all points on the two tangents to $\mathcal{A}^{(2)}$ which are in the 1-3 and 2-3 planes satisfy the equations $E_p=E_\phi=0$ identically. For $E\equiv E(p)$ one recovers

$$\mathcal{A}^{(1)}=\{-f''(p)(1-p^2)^{3/2} \ , f'(p)-f''(p)p(1-p^2)\} \ .$$

The static hysteresis loop discussed above neglects relaxation effects and does not allow one to study the temperature-dependent dynamic response of the system. Let us therefore address now a dynamic hysteresis loop based on the coherent rotation model. The problem is of considerable practical interest and a number of approximate model treatments exists.[18] Our discretization procedure leads to an *ab initio* expression for the nonequilibrium magnetization in the time-varying magnetic field. The theory has a number of applications which are briefly discussed in the conclusion to this section and in the next one where we present a calculation of the switching-field distribution.

We shall assume that at constant temperature the applied field varies with time according to $B=B(t)$ and that the inverse $t=t(B)$ exists. Typically $B(t)$ is a periodic function whose inverse is defined only piecewise on every half-period and this restricts our description of the hysteresis loop to one branch at a time. The discretization procedure is essentially the same as in the previous section and we write directly

$$\hat{P}(B,B_0)=P(T,B)+[P_{\mathrm{in}}-P(T,B_0)]e^{-\varepsilon(B,B_0)} -\int_{B_0}^{B}dB'\frac{\partial P(T,B')}{\partial B'}e^{-\varepsilon(B,B')} \ , \quad (22)$$

where $B_0=B(t_0)$ is the initial applied field and the function ε is defined by the integral

$$\epsilon(B,\bar{B})=\int_{\bar{t}}^{t}dt'\Gamma[T,B(t')]$$

$$=\int_{\bar{B}}^{B}dB'\frac{\partial t(B')}{\partial B'}\Gamma(T,B') \ . \tag{23}$$

In Eq. (22) we introduced the normalized probability distribution $\hat{P}$ which evolves at constant temperature in the time-varying magnetic field. The derivative in (22) is easily calculated: $\partial P/\partial B=T^{-1}(\langle E'\rangle_B-E')P$, where now $E'=\partial E/\partial B$. In hysteresis measurements $P_{\rm in}$ is usually the equilibrium state at $B=B_0$, $P_{\rm in}=P(T,B_0)$, e.g., at the origin of the virgin curve or at high saturation. The second term of Eq. (22) then vanishes. The equation for any branch of the hysteresis loop is given by $\tilde{M}(B,B_0)=V^{-1}\tilde{m}(B,B_0)$, where the magnetic moment is

$$\hat{m}(B,B_0)=\langle m\rangle_B+[\langle m\rangle_{\rm in}-\langle m\rangle_{B_0}]e^{-\epsilon(B,B_0)}$$

$$-\int_{B_0}^{B}dB'\frac{\partial\langle m\rangle_{B'}}{\partial B'}e^{-\epsilon(B,B')} \tag{24}$$

and

$$\partial\langle m\rangle_B/\partial B=T^{-1}[\langle E'\rangle_B\langle m\rangle_B-\langle mE'\rangle_B] \ .$$

Same as in the preceding section, the integrals over history are done over a product of two well-defined functions which, unfortunately, can only be done numerically even for the simple model (4). There is no need, however, to carry out numerical differentiation since all requisite derivatives are expressed in terms of easily calculated thermal averages.[19]

Equation (24) lends itself well to the study of hysteresis effects. We have employed[10] it, using model (4) with $\psi=0$, to calculate the coercivity $B_c(f,T)$ as a function of applied field frequency f and temperature T. As a special refinement of the method we included (approximately) backscattering effects by considering the net flux over the barrier, i.e., both to and from the initially overpopulated well. Equation (24) has a wide range (in temperature and frequency) of validity and we found that there exist two distinct relaxation regimes of the nonstationary process: The prefactor dominated regime at high temperatures where coercivity is but weakly T dependent and the Arrhenius factor dominated regime (low T) in which coercivity depends strongly on both temperature and sweep rate (see Fig. 1). The influence of T-dependent anisotropy and magnetization on coercivity was studied in Ref. 11 together with the possibility of experimentally observing temperature dependence of the decay rate prefactor. Our model makes it possible to easily accumulate large arrays of hysteresis curves and we used[12] it to calculate the coercivity of an ensemble of aligned uniaxial particles ($\psi=0$) with log-normal volume distribution and of misaligned particles ($0\le\psi\le\pi/2$) with $\cos^n\psi$ angular distribution. The possibility of applying our theory to clusters[20] of interacting particles with multiple relaxation channels is currently under investigation. The applicability of our theory is not confined to models of coherent rotation: The distribution function $P(T,B)$ of Eq. (22) can also, e.g., refer to a domain wall in a (possibly) multistable rather then bistable) pinning field.[21]

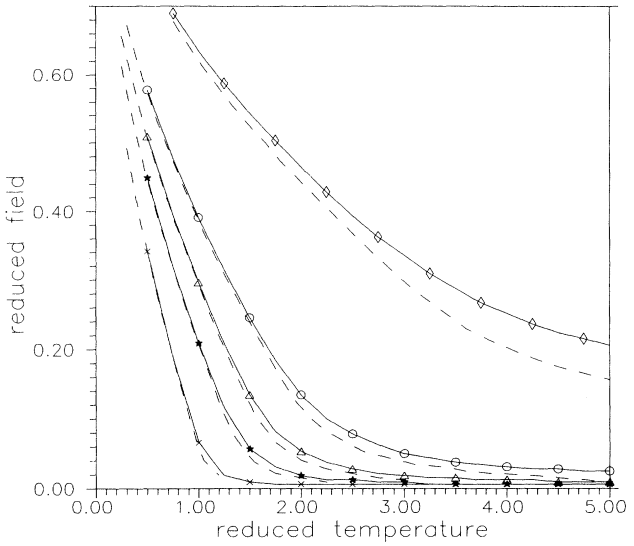

FIG. 1. The reduced coercivity $b_c=B_c(f,\vartheta)/B_N$ (solid lines) and the reduced field $b_\chi=B_\chi(f,\vartheta)/B_N$ (dashed lines) at which the susceptibility $\hat{\chi}[f,\vartheta|b,-1]$ has a maximum. The curves correspond to the sweep rates $f=10^2$ Hz ($\times$), 10^4 Hz ($*$), 10^5 Hz ($\triangle$), 10^6 Hz ($\circ$), and 10^8 Hz ($\diamond$).

V. SWITCHING FIELD DISTRIBUTION

In this section we apply Eq. (24) to calculate the switching-field distribution (SFD) of an array of the uniaxial particles (4) in parallel alignment with the field, $\psi=0$. For simplicity it shall initially be assumed that neither K nor M_s vary with temperature so that $b=B/B_N$ is independent of T. For our purposes only the barrier height $Q=KV$ in zero field is of relevance and we write $Q/T=(KV/T_A)\vartheta^{-1}$, where T_A is an arbitrary temperature. The value of the product KV/T_A is specified by demanding that $\Gamma^{-1}=1$ yr (we take $f_0=e^{25}$ Hz for the prefactor) at the reduced temperature $\vartheta=T/T_A=4\times10^{-1}$. In conclusion to this section, Eq. (27) below, we show how to relate these calculations to the temperature $\tau=T/T_C$.

The system is driven by the field $B(t)=-B_N\cos(2\pi ft)$ and at $t=0$ it finds itself by assumption in thermal equilibrium at $B=-B_N$, i.e., in the spin-down state. At given temperature ϑ and frequency f we calculate from Eq. (24) the nonequilibrium magnetization $\hat{M}[f,\vartheta|B(t),-B_N]$ for one half-sweep of the applied field on $t\in\langle 0,1/2f\rangle$. The coercivity $B_c(f,\vartheta)$ satisfies the equation $\hat{M}[f,\vartheta|B_c(f,\vartheta),-B_N]=0$ and the switching-field distribution is found by numerically differentiating the calculated hysteresis curves with respect to the instantaneous value of the applied field B at time t:

$$\hat{\chi}[f,\vartheta|B(t)]=\frac{\partial\hat{M}[f,\vartheta|B(t),-B_N]}{\partial B(t)}$$

$$\approx\frac{\Delta\hat{M}[f,\vartheta|B(t),-B_N]}{\Delta B(t)} \ . \tag{25}$$

For simplicity of notation we call these derivatives susceptibility.

We find that in the prefactor dominated region $\hat{\chi}$ approaches the reversible susceptibility $\chi_{\parallel}(\vartheta,b)$ discussed in conjugation with Eq. (9) whereas in the Arrhenius factor dominated region it is purely irreversible. At constant sweep rate f we plot the family of curves

$$\hat{\chi}_f(\vartheta|B)=\hat{\chi}[f,\vartheta|B(t)]|_{f=\text{const}}$$

versus the applied field B at selected values of temperatures. The nonequilibrium susceptibility $\hat{\chi}_f(\vartheta|B)$ attains its maximum value $\hat{\chi}_f(\vartheta|B_\chi)$ at the field $B=B_\chi(f,\vartheta)$ (Figs. 2 and 3). The curves $\{B_\chi,\hat{\chi}_f(\vartheta|B_\chi)\}$ have two local extrema (Fig. 4) which merge at very large f. It will be show that this complex structure is due to a transition between the prefactor and Arrhenius factor dominated relaxation regimes. The distinction between them vanishes at very high sweep rates. In the transition region the peak value $\hat{\chi}_f(\vartheta|B_\chi)$ of susceptibility *increases* with temperature while in the two limiting regions it *decreases* as expected. The isothermal remanent magnetization (IRM) susceptibility (SFD) is measured at very low sweep rates (large, but not well-defined waiting times between successive applications of the reversing field) and its temperature dependence[22] suggests that it corresponds to this transition region.

These model calculations have been carried out for sweep rates $f=10^0-10^8$ Hz and reduced temperatures $\vartheta\in\langle 0.25,5.5\rangle$. A representative sample of the resultant families of susceptibility curves $\hat{\chi}_f(\vartheta|B)$ is presented in Figs. 2 and 3 for $f=10^0$ Hz on the interval $\vartheta\in\langle 0.3,0.9\rangle$ and for $f=10^4$ Hz on $\vartheta\in\langle 0.25,2.25\rangle$. The temperature range for either frequency was chosen so as to include both the very rapidly and very slowly (with respect to f) switching regimes. The corresponding inverse decay rates are $\Gamma^{-1}(0.3,0)\approx 1.3\times 10^6$ yr, $\Gamma^{-1}(0.9,0)\approx 2\times 10^{-3}$ s, $\Gamma^{-1}(0.25,0)\approx 1\times 10^{11}$ yr, and $\Gamma^{-1}(2.25,0)\approx 2.5\times 10^{-8}$ s.

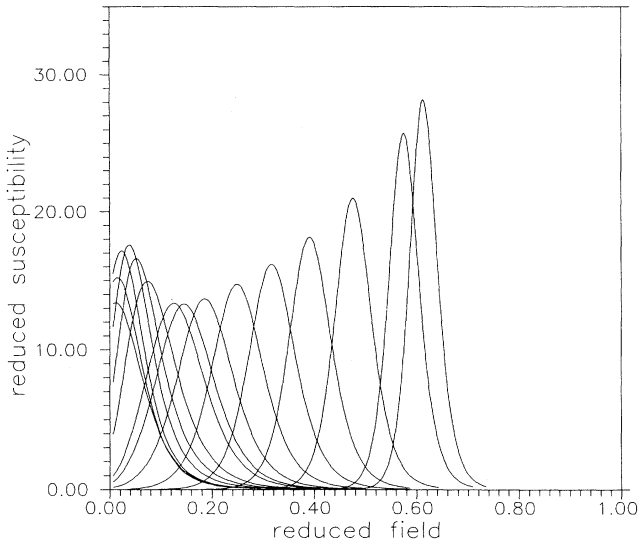

FIG. 3. The reduced susceptibility $(B_N/M_s)\hat{\chi}[f,\vartheta|b,-1]$ for $f=10^4$ Hz and $b=B/B_N>0$ at selected reduced temperatures ϑ: The rightmost curve corresponds to $\vartheta=0.25$, the leftmost one to $\vartheta=2.5$, the intervals $\Delta\vartheta$ are irregular.

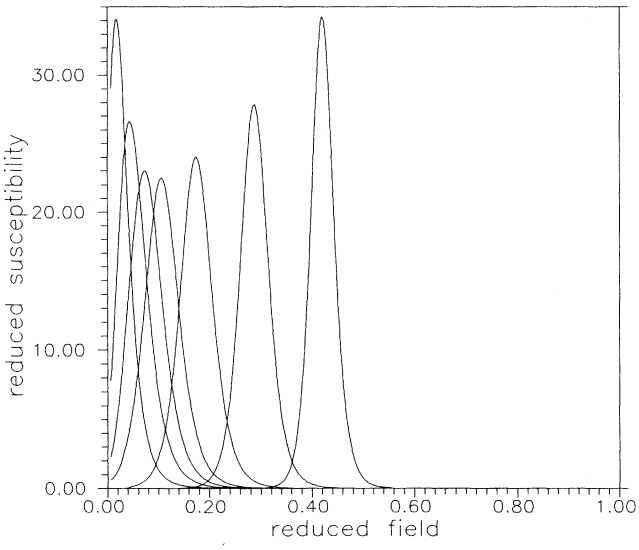

FIG. 2. The reduced susceptibility $(B_N/M_s)\hat{\chi}[f,\vartheta|b,-1]$ for $f=10^0$ Hz and $b=B/B_N>0$ at selected reduced temperatures ϑ. The functions $\hat{\chi}$ attain, at a given ϑ, a maximum at the field $b=b_\chi(f,\vartheta)$. The rightmost curve corresponds to $\vartheta=0.3$, the leftmost one to $\vartheta=0.9$, the intervals $\Delta\vartheta$ are irregular. Higher-temperature results could not be obtained with sufficient accuracy (compare Fig. 3).

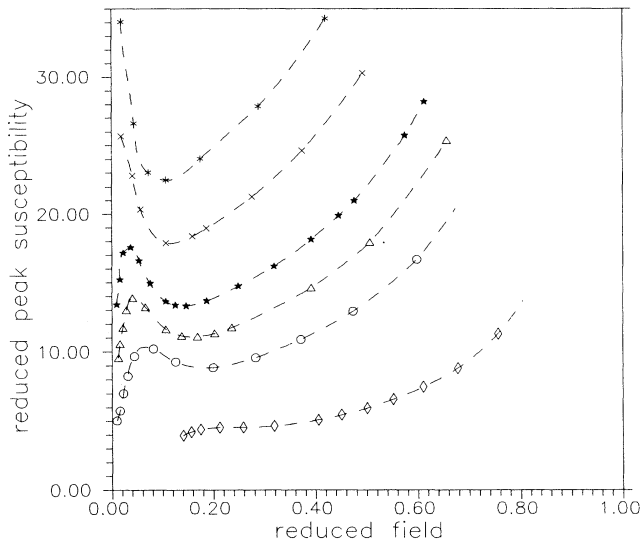

FIG. 4. The peak values of reduced susceptibility $(B_N/M_s)\hat{\chi}_f(\vartheta|b_\chi)$ as functions of the reduced field b_χ at which $\hat{\chi}$ has a peak. Temperature increases along each curve from right to left (see Fig. 5) and the sweep rates are 10^0 Hz (*), $f=10^2$ Hz (×), 10^4 Hz (*), 10^5 Hz (△), 10^6 Hz (○), and 10^8 Hz (◇). The dashed lines merely guide the eye.

The curves $\hat{\chi}_f(\vartheta|B)$ have a single maximum at the point $B_\chi(f,\vartheta)$ and we begin our discussion by comparing the value of $B_\chi(f,\vartheta)$ with the coercive field $B_c(f,\vartheta)$ whose plot is shown in Fig. 1. It is seen that B_c is very close to B_χ yet consistently somewhat larger. We explain this as a backscattering effect[10] which slows down the net overbarrier relaxation rate as the reversing field is gradually increased during the sweep: At $B=-B_N$ virtually all particles are in the spin-down state. On the other hand, at $B=0$ there is equal probability of jump in either direction but the spin-down well may still be (depending on f) heavily overpopulated while the spin-up well is almost empty. The net flux therefore goes from spin-down to spin-up states. Close to the coercive field, $B\approx B_c>0$, the two populations are almost equal and despite the biasing field there does exist a reverse flux, in particular, at low bias (small B_c or high temperature). The maximum relation rate is therefore attained somewhat earlier than coercivity.[23] Beyond coercivity, at very high fields $B\approx B_N$, the reverse flux cancels the net overbarrier flux altogether and detailed balance $(n_1\Gamma_{1\to2}=n_2\Gamma_{2\to1}$, where n_i are the populations in the two wells) is established. The disparity between B_c and B_χ is enhanced by increased temperature which, apparently, reduces the biasing effect of the applied field.

Let us now address the most prominent feature of graphs 2 and 3, to wit, the variation of the susceptibility peak value $\hat{\chi}_f(\vartheta|B_\chi)$ with temperature. Figure 4 shows the loci of points $\{B_\chi,\hat{\chi}_f(\vartheta|B_\chi)\}$ for six values of the sweep rate f. These are one-parametric curves in which the parameter (temperature) increases from right to left. The values of $\hat{\chi}_f(\vartheta|B_\chi)$ plotted as functions of temperature, $\{\vartheta,\hat{\chi}_f(\vartheta|B_\chi)\}$, are shown in Fig. 5, the one parameter of these curves being B_χ. Also shown in this figure is the equilibrium susceptibility $\chi_\parallel(\vartheta,0)$ in zero field. These two plots clarify the origin of the extrema in the peak value of susceptibility: As temperature is increased the values of both B_c and B_χ decreases until at sufficiently high temperatures the nonequilibrium curve $\hat{M}$ runs almost parallel to the equilibrium curve $\langle M\rangle_B$ a small distance away from it. Further increase in temperature has but scant effect on the already low values of B_c and B_χ but $\chi_\parallel(\vartheta,0)$ rapidly decreases to zero. This is manifest in Fig. 5 where the loci of points $\{\vartheta,\hat{\chi}_f(\vartheta,B_\chi)\}$ first rise to meet the limiting curve $\chi_\parallel(\vartheta,0)$ and then follow it to zero. In a very slow sweep this quasiequilibrium regime is reached at low temperatures for which $\chi_\parallel(\vartheta,0)$ is large. Within the precision of our calculation we could not numerically differentiate the rapidly varying (near zero field) 10^0- and 10^2-Hz hysteresis loops but there is no doubt that the corresponding two curves in Figs. 4 and 5 attain a maximum and turn subsequently to zero. An interesting feature is the virtual absence of local extrema at very high frequencies (here 10^8 Hz) where coercivity approaches zero only at high temperatures for which $\chi_\parallel(\vartheta,0)$ is small. In slow sweeps one can thus distinguish in Fig. 5 an initial low-temperature region of irreversible susceptibility and a high-temperature region where susceptibility is essentially reversible. In both of these regions the peak value of $\hat{\chi}_f(\vartheta|B_\chi)$ decreases with temperature while in the transition region it increases. The sharp segregation of the reversible and irreversible domains vanishes at high sweep rates. The effect is also observable in Fig. 1 where low-frequency coercivity has a distinct kink absent at high f.

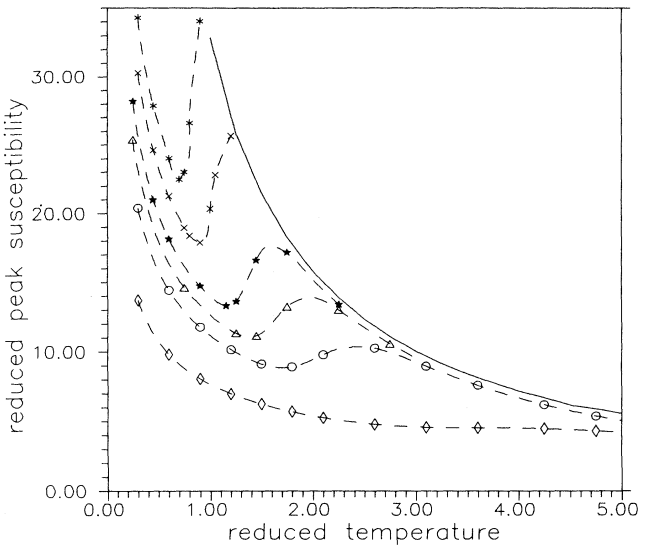

FIG. 5. The same peak values of reduced susceptibility as shown in Fig. 4, but plotted vs the reduced temperature ϑ. The solid line denotes equilibrium susceptibility $\chi_\parallel(\vartheta,0)$ at zero field. The tail section of the $f=10^0$- and 10^2-Hz curves could not be calculated with sufficient accuracy.

The remaining features of our graphs are as expected: At constant temperature susceptibility becomes more sharply peaked at small f since, upon reaching a low enough barrier height Q, the system has sufficient time to appreciably relax while Q (and the applied field) change but a little. A similar argument also holds for the broadening of $\hat{\chi}_f(\vartheta|B)$ with increasing temperature: At very low ϑ the decay rate is essentially zero for $B<B_c$ and then grows rapidly for $B>B_c$. On the other hand, at high temperatures $\Gamma(\vartheta,B)$ varies slowly with B so that relaxation begins at smaller fields and persists over a longer interval.

The low-temperature property of the decay rate makes it possible to estimate low-temperature coercivity $B_c=b_cB_N$ by demanding[24] that $\mathcal{Z}f=\Gamma(T,B_c)$, where for system (4) with $\psi=0$ Sharrock's formula $(1-b_c)^2=(T/KV)\ln(f_0/\mathcal{Z}f)$ follows, the proportionality constant $\mathcal{Z}$ turning out to be on the order of unity. This formula allows one to estimate the peak value of the purely irreversible susceptibility $\hat{\chi}_f(\vartheta|B_\chi)\approx\hat{\chi}_f(\vartheta,B_c)$ at low T and f. To this end we write approximately

$$M(t)=-2M_se^{-\Gamma(t)t}+M_s$$

in the vicinity of B_c. $\Gamma(t)$ is here a time-varying relaxation rate,

$$\Gamma(t)=f_0\exp[-(KV/T)\{1+\cos(2\pi ft)\}^2]\ .$$

For $B\neq\pm B_N$ there is

$$\partial/\partial B = B_N^{-1}(2\pi f \sin 2\pi f t)^{-1}\partial/\partial t$$

and therefore

$$\left.\frac{\partial M(t)}{\partial B}\right|_{B_c} \approx 4\frac{M_s}{B_N}\frac{KV}{T}(1-b_c)\Gamma(t)te^{-\Gamma(t)t}\Big|_{t=t(B_c)} \propto \frac{M_s}{B_N}\left[\frac{KV}{T}\ln\frac{f_0}{Zf}\right]^{1/2}. \quad (26)$$

We assumed here that $(1-b_c)KV/T \gg 1$, used Sharrock's formula for B_c, and set the product $\Gamma te^{-\gamma t} \approx 1$. The temperature dependence of this formula is not easily verified because of its limited validity but the predicted frequency dependence corresponds to our Figs. 4 and 5. To see this let $Zf = e^{\sigma}$. Then

$$\partial M/\partial B \propto \ln^{1/2}\{f_0/(Zf)\} \approx 5(1-\sigma/50)$$

decreases linearly with small σ. In our case deviations are observed only at the 10^8-Hz curve.

Temperature dependence of the magnetic parameters K and M_s given by Eqs. (1) and (2) may be included by the following argument: We have chosen the arbitrarily scaled temperature $\vartheta = T/T_A$ to label our graphs but this way of labeling is a mere matter of convention. There exists (at fixed KV/T_A) a one-to-one correspondence between ϑ and Γ and we could just as well label our graphs by the decay rate in zero field (or any other field, for that matter). We can therefore establish a correspondence between $\vartheta = T/T_A$ and $\tau = T/T_C$ introduced in Eq. (1) by demanding that

$$\Gamma(\vartheta,0) = \Gamma(\tau,0) \Longrightarrow \tau = \vartheta q_C/(\vartheta q_C + q_A). \quad (27)$$

In this equation $q_A = KV/T_A$ and $q_C = K(0)V/T_C$ for brevity. The value of q_A has been fixed for our graphs previously by setting $\Gamma^{-1}(0.4,0) = 1$ yr and q_C may now be chosen at will. The reduced field $b = B/B_N \rightarrow b(\tau) = B/B_N(\tau)$ of Eq. (5). To every $B = bB_N$ of our graphs there corresponds therefore the field $B(\tau) = B[B_N(\tau)/B_N] < B$. Equation (27) merely relabels our graphs and the subsequent rule results in a nonlinear contraction of the B axes.

In conclusion let it yet be remarked that the inequality $\partial\langle M\rangle_B/\partial B > \partial\hat{M}/\partial B$ holds at arbitrary temperature since any system shall relax more during an infinite time than during a finite time interval. This purely thermodynamic property explains the existence of the limiting curve $\chi_{\parallel}(T,0)$ but the complicated structure of the region bridging the reversible and irreversible limits is model dependent and should, in our opinion, be also studied for other models. In particular, we conjecture that in multistable (rather than in bistable) systems the function $\chi_f(T|B_\chi)$ is likely to be very complex.

ACKNOWLEDGMENTS

One of us (I.K.) would like to thank the National Science Council of ROC for support under Grants Nos. NSC-81-0405-E002-13 and NSC-82-0208-M002-035.

[1] C. P. Bean, J. Appl. Phys. **26**, 1381 (1955).
[2] O. Popov and M. Mikhov, J. Magn. Magn. Mater. **82**, 29 (1989).
[3] O. Popov, P. Rachev, M. Mikhov, F. Calderon, J. L. Sanchez Ll., and F. Leccabue, J. Magn. Magn. Mater. **99**, 119 (1991).
[4] O. Popov and M. Mikhov, J. Magn. Magn. Mater. **75**, 135 (1988).
[5] R. W. Chantrell, M. El-Hilo, and K. O'Grady, IEEE Trans. Magn. MAG-**27**, 3570 (1991).
[6] D. H. Reich, B. Ellman, J. Yang, T. F. Rosenbaum, G. Aeppli, and D. P. Belanger, Phys. Rev. B **42**, 4631 (1990).
[7] M. Escorne, A. Mauger, V. Paul-Boncour, and A. Percheron-Guegan, Solid State Commun. **76**, 757 (1990).
[8] S. B. Oseroff, D. Franks, and V. M. Tobin, IEEE Trans. Magn. MAG-**23**, 2871 (1987); V. M. Tobin, S. B. Oseroff, S. Schultz, and M. P. Sharrock, *ibid.* **MAG-25**, 3653 (1989). The authors quote the value of $KV = 10^{-11}$ erg as the basis of their numerical simulation. This must be a misprint since the corresponding decay rate in zero field is $\sim\exp(-10^3) \approx 10^{-400}$ at room temperature and coercivity and nucleation field would be indistinguishable.
[9] P. J. Flanders and M. P. Sharrock, J. Appl. Phys. **67**, 2918 (1987).
[10] H. L. Huang, I. Klik, C. R. Chang, and K. K. Liang, Proceedings of the MRM '92 Conference, Perugia, Italy [J. Magn. Magn. Mater. (to be published)].
[11] I. Klik, Proceedings of the MMM '92 Conference, Houston, Texas [J. Appl. Phys. (to be published)].
[12] I. Klik, H. L. Huang, and C. R. Chang, Proceedings of the MMM'92 Conference, Houston, Texas [J. Appl. Phys. (to be published)].
[13] I. Klik and L. Gunther, J. Appl. Phys. **67**, 4505 (1990).
[14] I. Klik and L. Gunther, J. Stat. Phys. **60**, 473 (1990); I. Klik, *ibid.* **66**, 635 (1992).
[15] A fuller description taking into account one or more intermediate states is obtained from a master equation, see, e.g., H. Pfeiffer, Phys. Status Solidi A **122**, 377 (1990).
[16] J. I. Gittelman, B. Abeles, and S. Bozowski, Phys. Rev. B **9**, 3891 (1974).
[17] G. Xiao, S. H. Liou, A. Levy, J. N. Taylor, and C. L. Chien, Phys. Rev. B **34**, 7573 (1986); G. Xiao and C. L. Chien, Appl. Phys. Lett. **51**, 1280 (1987).
[18] F. Ossart and G. Meunier, IEEE Trans. Magn. **MAG-26**, 2837 (1990); D. C. Jiles and J. B. Thoelke, *ibid.* **MAG-25**, 3928 (1989).
[19] In the asymptotic limit all averages are, of course, done easily. For the Hamiltonian (4) it is also possible to express them in terms of incomplete error functions, see W. Magnus, F. Oberhettinger, and R. P. Soni, *Formulas and Theorems for the Special Functions of Mathematical Physics* (Springer, Berlin, 1966), Sec. 9.1.2.
[20] W. Chen, S. Zhang, and N. H. Bertram, J. Appl. Phys. **71**, 5579 (1992).
[21] J. F. Liu and H. L. Luo, J. Magn. Magn. Mater. **94**, 43 (1991).
[22] G. W. D. Spratt, P. R. Bissell, R. W. Chantrell, and E. P. Wohlfarth, J. Magn. Magn. Mater. **75**, 309 (1988); R. W. Chantrell, *ibid.* **95**, 365 (1991).
[23] We found, however, no published experimental data to support this conjecture.
[24] M. P. Sharrock, IEEE Trans. Magn. **MAG-26**, 193 (1990).